The Hubble constant and Virgo cluster distance from observations of Cepheid variables

Michael J. Pierce*†‡, Douglas L. Welch†§, Robert D. McClure†‖, Sidney van den Bergh‖, René Racine†¶ & Peter B. Stetson‖

* Kitt Peak National Observatory, National Optical Astronomy Observatories, PO Box 26732, Tucson, Arizona 85726, USA
§ Department of Physics and Astronomy, McMaster University, Hamilton, Ontario L8S 4M1, Canada
‖ Dominion Astrophysical Observatory, Herzberg Institute of Astrophysics, National Research Council, 5071 W. Saanich Road, Victoria, British Columbia V8X 4M6, Canada
¶ Département de Physique, Université de Montréal, C. P. 6128 Succ. A., Montréal, PQ H3C 3J7, Canada

The distance to the Virgo cluster of galaxies, a primary rung on the ladder to establishing the distance scale of the Universe, 14.9 ± 1.2 Mpc, has been determined through ground-based observations of Cepheid variables in NGC4571. This agrees very well with other modern distance estimates, and the extragalactic distance scale now seems established. Based on this distance, a Hubble constant of $H_0 = 87 \pm 7$ km s^{-1} Mpc^{-1} has been calculated.

IMPORTANT and rapid progress is being made in establishing the extragalactic distance scale. The more modern and quantitative methods have now been defined and applied to a significant number of galaxies, so that an intercomparison and testing of these methods is now possible[1-3]. The result is that these methods are all in good agreement, with the exception of type Ia supernovae (SN Ia) as calibrated by Sandage[4,5]. However, SN Ia may not be as uniform as previously claimed[6] and there may be notable problems in the photometry of the calibrating events[7], such that the discrepancy may not be as significant as is often claimed. This discrepancy has led to the well known dispute about the absolute distance scale in the Universe, which is frequently characterized as a debate over the value of the Hubble constant.

It is now generally accepted that the discrepancy between the 'short' ($H_0 = 80$–100 km s^{-1} Mpc^{-1}) and 'long' ($H_0 = 50$ km s^{-1} Mpc^{-1}) distance scales begins rather abruptly at a distance of about 7 Mpc (refs 3, 8). That is, the distances to nearby galaxies are in good absolute agreement and the distances beyond about 7 Mpc are in good relative agreement. Similarly, it can be shown that the various values for H_0 found in the literature correlate strongly with the reported distance for the Virgo cluster in those same sources. Thus, establishing the value of H_0, to say 10%, can be done by establishing the distance to the Virgo cluster to a similar precision. This is the case even in the presence of significant large-scale peculiar velocities, as shown by the linearity of the Hubble diagram[9] using either brightest cluster members[10] or SN Ia (ref. 11).

The one method that has not been applied beyond 7.5 Mpc is also the one which holds the greatest promise in alleviating this discrepancy[1]. This is the use of the Cepheid period–luminosity relation. A Cepheid is a pulsating variable star whose pulsation period is strongly correlated with its luminosity. By determining a Cepheid's period, its luminosity is immediately known, allowing its distance to be determined from its apparent brightness. These stars are well understood from both empirical and theoretical perspectives and have an important and well tested history of application[12]. Consequently, it has been argued that the detection of Cepheid variables in the Virgo cluster is the best hope for establishing the extragalactic distance scale[13]. Historically, this has been thought to be beyond the capabilities of ground-based telescopes and thus was used as a prime example to justify the need for space-based science. However, the continuing progress in ground-based, high-resolution imaging has made the prospects for such a survey much more feasible[14].

We report here the results of such a survey, using the high-resolution camera (HRCam) on the Canada-France-Hawaii Telescope on Mauna Kea. We identified three probable Cepheid variables in an H I-depleted galaxy near the core of the Virgo cluster, and determined their periods. After correcting the apparent magnitudes of the Cepheids for extinction in the Milky Way along the line of sight to the Virgo cluster, we determined that the galaxy lies at a distance of 14.9 ± 1.2 Mpc. We have now established an absolute reference for the extragalactic distance scale. After correcting for the motion of the cluster with respect to the cosmic microwave background, we calculate a value for the Hubble constant, $H_0 = 87 \pm 7$ km s^{-1} Mpc^{-1}. This high value, in conjunction with most currently fashionable cosmological models, conflicts with the ages of the oldest known stars.

Cepheid variables in NGC4571

NGC4571 was chosen as a promising target for a variable star survey given the expected performance of the HRCam on the Canada-France-Hawaii Telescope. It is a moderate-luminosity spiral (Sbc II; ref. 15) with a correspondingly lower disk surface brightness such that it should resolve relatively easily into stars[16]. In addition, it is sufficiently luminous to contain a reasonable number of luminous Cepheids[14], of which we have isolated three. We first give arguments why we expect the distance of NGC4571 to be representative of the distance to the Virgo cluster.

NGC4571 is located less than 2.5° from M87 and shows signs of significant H I stripping[37]. This provides strong evidence for NGC4571 being in the 'core' of the Virgo cluster, given the extensive evidence for the occurrence of stripping within the cores of rich clusters and the fact that the Virgo spirals with significant stripping are within 3° of M87 (ref. 38). Because the mean heliocentric velocity of the Virgo cluster ellipticals and lenticulars is $\langle v_\odot \rangle = 1{,}045 \pm 63$ km s^{-1} with a radial velocity dispersion of $\sigma = 556$ km s^{-1} (ref. 17), the low radial velocity of NGC4571 (342 ± 3 km s^{-1}) is further evidence for this galaxy being in or near the dynamically relaxed core of the cluster. The line-of-sight velocities for any particular galaxy projected upon an over-dense region are 'triple-valued' in the predicted distance

† Visiting Astronomer, Canada-France-Hawaii Telescope.
‡ Present address: Department of Astronomy, Indiana University, Bloomington, Indiana 47405, USA.

using linear infall models of the cluster region[18]. However, when the velocities are low this ambiguity becomes minimal. For example, the Virgo-centric infall model of Tully and Shaya[19] predicts distances for NGC4571 of 3.6, 15.5 and 19.1 Mpc, if the Virgo cluster is at 15.5 Mpc. Although this particular model predicts an infall velocity for the Galaxy of 300 km s^{-1}, the predicted distances are relatively insensitive to the infall velocity of the Galaxy. The first possible distance is easily eliminated because, if this were the case, the galaxy would be unique in both absolute size and luminosity for its luminosity class[15] and would have been resolved into stars long ago. The second possibility is that the galaxy is in the core of the cluster, and the third is that NGC4571 is ~23% further away than the Virgo cluster 'core'. As we will soon demonstrate, the latter case will seem very unlikely given the distance we derive.

We acquired imaging observations of NGC4571 with HRCam at 13 epochs during the 1991, 1992 and 1993 seasons. HRCam is essentially a 'fast guider' which operates at frequencies of up to 200 Hz and is capable of correcting for the 'tip-tilt' component of atmospheric seeing by monitoring a nearby guide star. The characteristics of HRCam have been described in refs 20 and 21. A total of 75 usable images were acquired using the SAIC 1 and Loral 3 CCDs (charge-coupled devices) between 11 February 1991 and 27 April 1993. For each 'epoch', we typically took ~5, 15–20-min exposures in the R bandpass, shifting the image on the CCD by ~5 pixels between each to reduce the effects of cosmetic defects. The images were bias-subtracted and flat-fielded with a median of several twilight sky flats in the typical manner. The combined exposures of a given epoch produced an image with typical full-width half-maximum (FWHM) ~0.50 arcsec and a limiting magnitude of $R \sim 26$ mag. We also acquired 2 epochs in the V bandpass in order to measure $V-R$ colours for any variables we might find. The details of our observing procedures will be described in a separate paper (D.L.W. *et al.*, manuscript in preparation).

We obtained photometry of the resolved stars in NGC4571 via DAOPHOT/ALLFRAME[22,23]. ALLFRAME was ideal for our survey because it performs simultaneous point-spread function fitted photometry on multiple image frames using a 'master' list of program stars with fixed relative position. This 'master' list was obtained by running DAOPHOT II on an image constructed from the median of the 53 best (FWHM $\leqslant$0.55 arcsec) individual exposures (Fig. 1).

The identification of variables proceeded as follows. First, a weighted mean magnitude, $\bar{R}$, was determined for each night for each star. Global mean V magnitudes were also determined and hence a mean $(V-R)$ index was formed. Using the mean $(V-R)$, the photometry was brought onto the same scale by correcting the photometry for colour terms. Only the first two epochs were found to have significant colour terms as these were the epochs for which a non-standard '$V+R$' filter was used[24]. Once the photometry was corrected for the colour term, a variability index[25] was formed using four sets of adjacent epochs. Three of these sets contained pairs of epochs and one set contained a triplet of epochs. Because the actual form of the variability index used is different from that in ref. 25, it will be briefly described.

For each star, for each epoch i, the number of detections, n, is established. From the set of magnitudes $R_{i,j}$ and uncertainties $\sigma_{i,j}$ available at each epoch, the jth residual is

$$\delta R_{i,j} = \frac{R_{i,j} - \bar{R}}{\sigma_{i,j}} \quad (1)$$

For that epoch, the contribution to the variability index, $\mathscr{I}_i$, was calculated to be

$$\mathscr{I}_i = \frac{2}{n} \sum_{\substack{j=1,n-1 \\ k=j,n}} \text{sign}\,(\delta R_{i,j}\delta R_{i,k})\sqrt{\delta R_{i,j}\delta R_{i,k}} \quad (2)$$

where sign (. . .) has an absolute value of one and the sign of the argument. The form of the product of the residuals is different from that in ref. 25 in that it reduces the impact of one epoch of correlated residuals on the final statistic. The final variability index, $\mathscr{I}$, for the N epochs with useful correlated magnitude residuals was then found by calculating

$$\mathscr{I} = \sqrt{\frac{1}{N(N-1)}} \sum_{i=1,N} \mathscr{I}_i \quad (3)$$

At this point, it was determined that a major source of false variable identifications was due to stars within a few pixels of

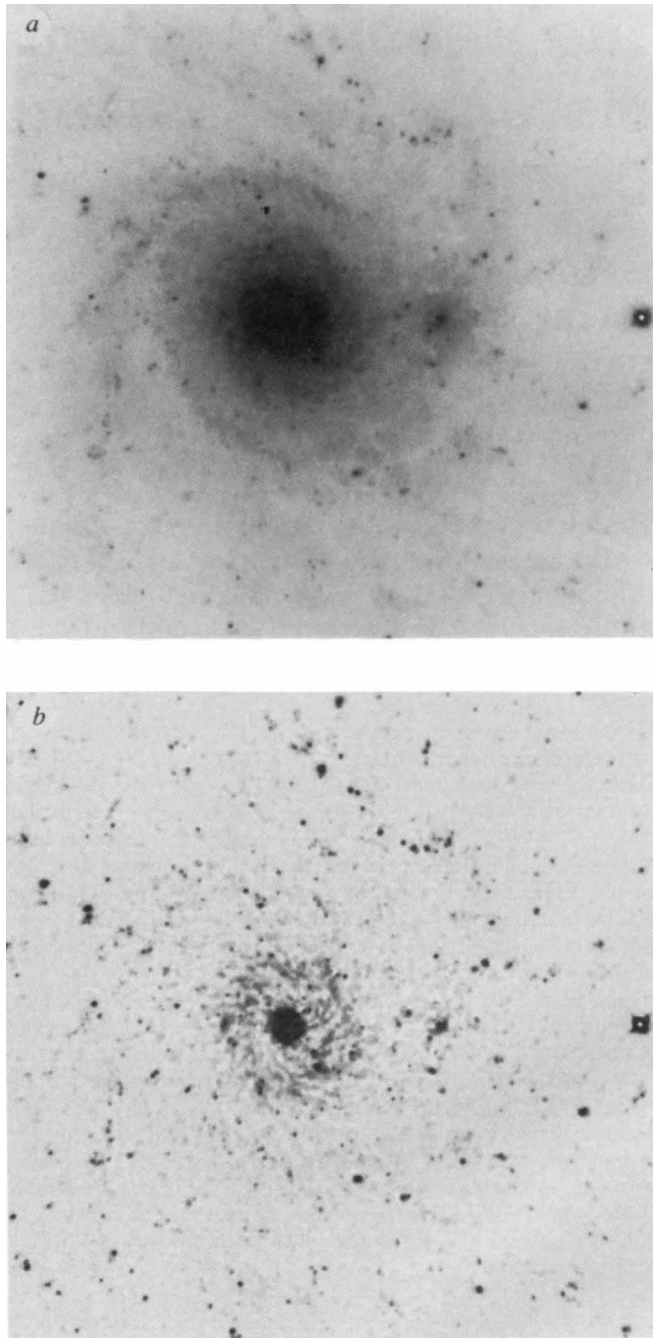

FIG. 1 *a*, A combination of 53 15–20-min exposures of NGC4571. The image has a FWHM = 0.49 arcsec and is ~150 arcsec on a side with 0.11 arcsec per pixel. *b*, The same image after a smoothed version of the residual image (with fitted stars subtracted) has been subtracted. The limiting magnitude of these images is $R \sim 28$. Note the numerous stars and star-forming regions.

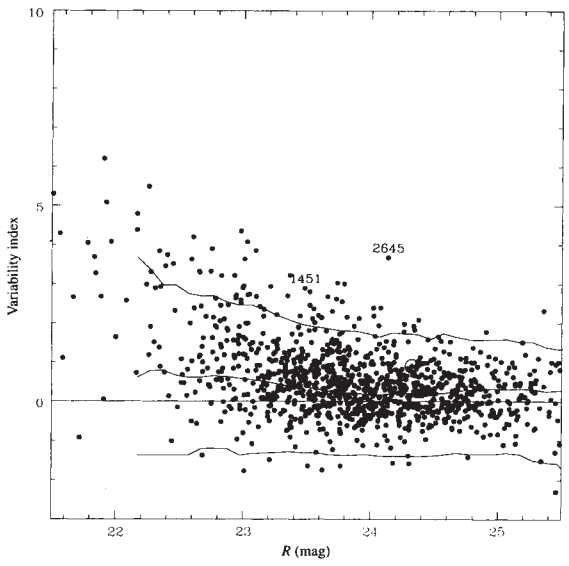

FIG. 2 The variability index[25] as a function of mean R magnitude. The three irregular curves indicate the 5th-, 50th- and 95th-percentiles of the variability index distribution as derived from the uncorrelated magnitude residuals of stars of similar brightness and crowding. Only stars further than 22 arcsec from the nucleus of NGC4571 were considered (see text). The three variables identified as Cepheids are indicated. Stars 1451 and 2645 were identified from their variability index, whereas star 2114 (the open circle within the general distribution) was identified from a visual examination of the photometry of the most isolated stars.

the CCD edge at more than one epoch, so potential variable candidates were checked for edge proximity on the original frames. Only stars with a full four sets of correlated epochs were considered further.

A plot of the variability index as a function of R magnitude appears in Fig. 2. In the absence of additional factors that might correlate magnitudes from different epochs (for example systematic flat-fielding errors, close companions and so on), the distribution should be symmetrical about zero. Although this is not strictly the case, for the reasons outlined above, we can still assess the significance of variability for any particular star. Stars with unusually large positive variability index values are probably variable stars. Figure 2 also displays confidence intervals for the 5th-, 50th- and 95th-percentile points of the distribution found using correlations formed from the residuals of different stars within 0.5 magnitudes of the abscissa. Several candidates clearly warrant further inspection. Stars above the 95th-percentile were examined for spurious 'variability' due to correlated photometry with close companions, background nebulosity and so on. Two stars were judged as genuine variables with lightcurves and periods (see below) consistent with Cepheids (1451 and 2645). In addition, we also did an independent visual examination of the photometry of all stars with $R \leqslant 25.0$ which were considered isolated (no companion within ~2× the FWHM). Although subjective, this approach also identified star 2645 as a variable and produced one additional candidate Cepheid, 2114.

Calibrations were computed from a variety of standard stars (refs 26, 27 and L. Davis, personal communication) which showed agreement to within 2%. The ALLFRAME photometry was referenced to these calibrations using large-aperture photometry of the brightest, isolated stars in the images. The non-photometric nights were referenced to these nights through a robust mean zeropoint determination for each epoch (DAOMASTER).

A form of the 'string length' technique for finding likely periods, called the Lafler–Kinman technique[28], was then used to search for likely periods. We present the Lafler–Kinman statistic[28] (Θ), and best-fit lightcurve for our candidate variables in Fig. 3*a–c*. Although minima in the Lafler–Kinman statistic are associated with the true period, additional spurious minima resulting from chance phase alignments of points and aliasing also occur. The minima due to aliasing are generally present in each of the plots such that these could be identified. Most of the additional spurious minima do not result in reasonable lightcurves when the data is phased with that trial period and can thus be eliminated as well. This procedure resulted in three stars

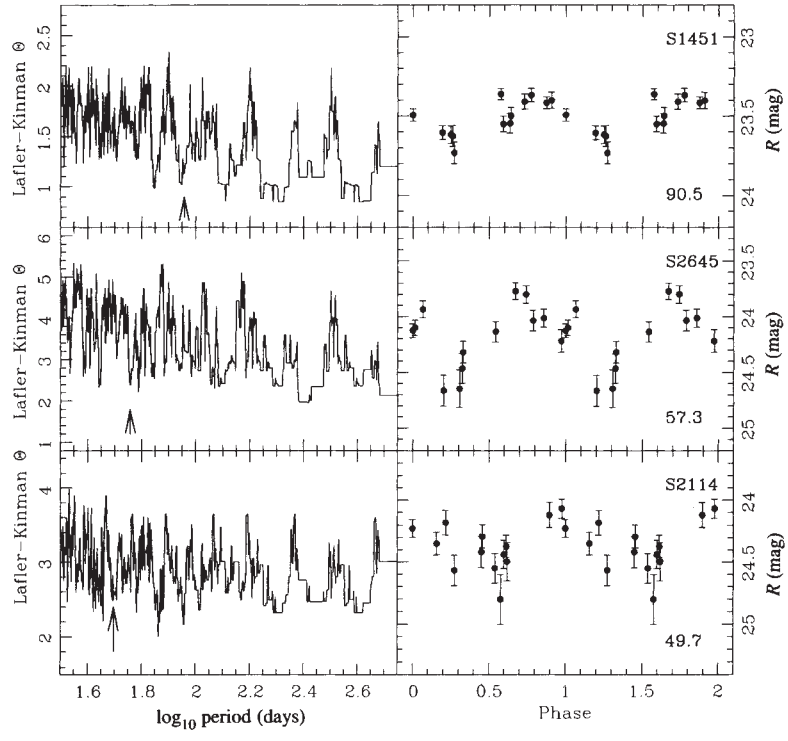

FIG. 3 The panels on the left show the Lafler–Kinman string length (Θ, see text) as a function of log(P) for each of the three candidate Cepheids. Note that aliases due to our limited number of epochs result in spurious features which generally repeat in each panel and can thus be eliminated from consideration. The adopted periods for each of the variables are indicated. The panels on the right illustrate the R-band light curves for the three candidate Cepheids with the periods given by the string length analysis. Each point is shown twice to allow continuity through zero phase to be assessed.

TABLE 1 Cepheid variables in NGC4571

Identification	$\log_{10} P$	$\langle R \rangle$ (mag)	$V-R$*	$m-M$†
2114‡	1.696	24.33	0.2	30.93
2645	1.759	24.14	0.5	30.93
1451	1.954	23.48	0.0	30.86

* We assign an uncertainty of ±0.15 mag to the $V-R$ colours given the small number of epochs (two) for which we acquired V photometry.

† The apparent distance modulus (in mag) based on the LMC calibration[12] that assumes an LMC modulus of 18.5 mag.

‡ A less certain variable selected from a visual examination of the photometry of the most isolated stars.

we concluded to be Cepheids (see Fig. 3). The photometry of these stars and their periods are given in Table 1, and are shown graphically in Fig. 4. We note that although the $V-R$ colours are uncertain they are sufficiently accurate to eliminate the possibility that these variables might be long-period variables, which have much redder colours ($V-R \approx 1.0$) than Cepheids ($V-R \approx 0.5$).

P–L relationship and the distance to NGC4571

We now use the periods of the identified Cepheids to determine the distance of NGC4571. The period determines the absolute magnitude (luminosity) of each star, and we combine the results from all three to reduce the final uncertainty. After correcting the observed brightnesses for extinction from dust within the Milky Way, we calculate a distance of 14.9 ± 1.2 Mpc, which we take as the distance of the centre of the Virgo cluster.

It is apparent from Table 1 that only Cepheids over a relatively narrow range in period have been detected. Consequently, we followed the usual procedure of adopting the slope and zero-point of the P–L relationship for Cepheids in the Large Magellanic Cloud (LMC) and computed the best-fitting relative distance modulus (Fig. 4). We adopt the calibration in ref. 12, assuming a distance modulus of 18.5 mag for the LMC; $M_R = -3.04[\log_{10}(P) - 1.0] - 4.48 \pm 0.08$ mag, where the period (P) is in days. The resulting apparent distance modulus for each variable was computed and is also given in Table 1. We find a mean apparent modulus for NGC4571 of $(m-M)_A = 30.91 \pm 0.15$ mag, where the uncertainty resulting from the finite width of the instability strip ($\sigma = 0.2$ mag; ref. 12) and that of the distance to the LMC contribute equally. This value must be corrected for any extinction by dust along the line-of-sight to the Cepheids in NGC4571. The extinction within our own Galaxy in the direction of NGC4571 is $A_B = 0.07$ mag (ref. 29), which corresponds to $A(R) = 0.04$ mag, assuming a standard reddening law. Although there is likely to be some additional internal extinction within NGC4571 we cannot estimate this accurately given the limited precision in our colours for the Cepheids. However, the colour of the 'plume' brightest blue supergiants[24] suggests little reddening. Therefore, we assume no additional extinction for the Cepheids in NGC4571 and adopt $(m-M)_0 = 30.87 \pm 0.15$ mag. The corresponding distance is 14.9 ± 1.2 Mpc, assuming that NGC4571 is within the 3° core of the Virgo cluster.

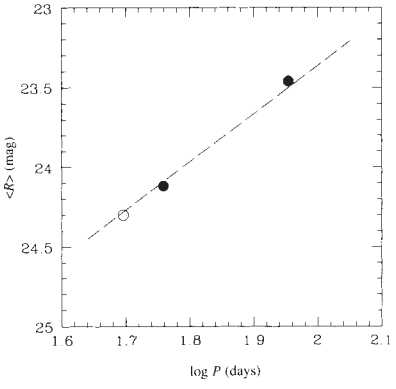

FIG. 4 The period–luminosity relationship for the Cepheids in NGC4571 and the mean relation for those in the LMC assuming $(m-M)_{LMC} = 18.5$ (dashed line). The solid points indicate those variables indentified from the variability index (see Fig. 3 and text), and the open point indicates the additional variable (2114) found from an independent examination of the photometry of the most isolated stars. The adopted apparent distance modulus of $(m-M)_A = 30.91 \pm 0.15$ is derived from the mean of the three variables.

We now consider two potential biases which might effect the distance we derived above. First, the effects of crowding will tend to bias the mean magnitudes too bright. That is a superimposed companion of similar brightness to the Cepheid will contaminate the photometry of the Cepheid. However, the presence of an undetected companion will also reduce the apparent amplitude of the Cepheid. For example, let us assume the Cepheids have an actual amplitude (in R) near the maximum found for those in the Large and Small Magellanic Cloud, with similar periods (0.3–0.7 mag; ref. 30). The observed amplitudes we find are 0.7, 0.5 and 0.3 for stars 2645, 2114 and 1451, respectively. Thus we can place limits of 0.0, 0.5 and 0.6 mag on the maximum contamination of these stars. The bluer colours of the latter two might be considered as evidence for contamination but the colours are rather uncertain. So, while we cannot rule out as much as 0.5 mag of contamination for two Cepheids, it must be pointed out that the luminosities of the contaminating stars would be extreme ($M(V) \approx -6.8$) and such stars are exceedingly rare. Furthermore, it would remain a mystery why we obtain the same distance for NGC4571 with these 'contaminated' Cepheids as we get using star 2645, which cannot be significantly contaminated. So, although we concede that contamination is possible we have no evidence of any contamination by close companions and we therefore make no correction to the estimated distance of NGC4571. A second potential bias has been argued to result from the finite width of the P–L relationship coupled with a small range in sampled period. This is sometimes claimed to result in a selection bias such that the brightest variables at a given period will be preferentially detected in a magnitude limited survey. We only point out that the dispersion of the relation at R is only 0.25 mag (ref. 30) and any bias that might result is minimal.

The Hubble constant

As argued above, the estimated distance for NGC4571 is very probably appropriate to the core of the Virgo cluster itself. In fact, this estimate agrees with the majority of other methods currently in use[1]. Consequently, we consider this result a verification of these methods and it lends strong support to the view that the extragalactic distance scale is now established. Although one could argue that NGC4571 just happens to lie in the foreground of the Virgo cluster, such an argument seems extremely *ad hoc* given the evidence that NGC4571 is in or near the core of the cluster. The implications of such a 'short' distance scale are well known. Given that the relative distances between the Virgo cluster and more distant clusters are in good agreement we can compute the Hubble constant from the distance given above. We adopt a relative distance modulus between the Virgo and Coma clusters of $\Delta m = 3.71 \pm 0.05$ mag (refs 31–34) and a mean velocity for Coma of $\langle v_\odot \rangle = 6{,}888 \pm 86$ km s^{-1} (ref. 35). With an additional correction of 258 ± 10 km s^{-1} to place Coma in the reference frame of the CMB we find that

$$H_0 = 87 \pm 7 \text{ km s}^{-1} \text{ Mpc}^{-1} \quad (4)$$

This estimate assumes that no additional correction to the velocity of the Coma cluster is necessary because of peculiar motion. However, this value is likely to be representative over large scales given that there is no evidence for very large streaming motions out to scales of several hundred Mpc (refs 9, 10). The corresponding expansion ages for the Universe are

11.2 ± 0.9 Gyr and 7.3 ± 0.6 Gyr for $\Omega = 0$ and 1, respectively. These values are well known to be in conflict with the estimated ages for metal-poor Galactic globular clusters (for example 16.5 ± 2 Gyr; ref. 36) and an inflationary cosmology with zero cosmological constant. The origin of this apparent paradox does not appear attributable to the observational data. □

Received 26 August; accepted 19 September 1994.

1. Jacoby, G. H. *et al. Publs astr. Soc. Pacif.* **104,** 598 (1992).
2. Ciardullo, R., Jacoby, G. H. & Tonry, J. L. *Astrophys. J.* **419,** 479 (1993).
3. Pierce, M. J. *Astrophys. J.* **430,** 53 (1994).
4. Sandage, A., Saha, A., Tammann, G. A., Panagia, N. & Macchetto, F. D. *Astrophys. J.* **401,** L7 (1992).
5. Sandage, A. *et al. Astrophys. J.* **423,** L13 (1994).
6. Phillips, M. M. *Astrophys. J.* **413,** L105 (1993).
7. Pierce, M. J. & Jacoby, G. H. *Astr. J.* (submitted).
8. de Vaucouleurs, G. *Astrophys. J.* **415,** 10 (1993).
9. Sandage, A. & Tammann, G. A. *Astrophys. J.* **365,** 1 (1990).
10. Lauer, T. R. & Postman, M. *Astrophys. J.* **400,** L47 (1992).
11. Hamuy, M. *et al. Astr. J.* (submitted).
12. Madore, B. F. & Freedman, W. L. *Publs astr. Soc. Pacif.* **103,** 933 (1991).
13. Sandage, A. *Proc. 12th Aerospace Sciences Meeting* (ed. Simmons, F. P.) 19 (American Institute of Aeronautics and Astronautics, New York, 1974).
14. Pierce, M. J., McClure, R. D. & Racine, R. *Astrophys. J.* **393,** 523 (1992).
15. van den Bergh, S., Pierce, M. J. & Tully, R. B. *Astrophys. J.* **359,** 4 (1990).
16. Sandage, A. & Bedke, J. *An Atlas of Galaxies Useful for Measuring the Cosmological Distance Scale* (NASA SP-496, Washington, 1988).
17. Binggeli, B., Tammann, G. A. & Sandage, A. *Astr. J.* **94,** 251 (1987).
18. Davis, M. & Peebles, P. J. E. *A. Rev. Astr. Astrophys.* **21,** 109 (1983).
19. Tully, R. B. & Shaya, E. J. *Astrophys. J.* **281,** 31 (1984).
20. Racine, R. & McClure, R. D. *Publs astr. Soc. Pacif.* **101,** 731 (1989).
21. McClure, R. D. *et al. Publs astr. Soc. Pacif.* **101,** 1156 (1989).
22. Stetson, P. B. *Publs astr. Soc. Pacif.* **99,** 191 (1987).
23. Stetson, P. B. *Publs astr. Soc. Pacif.* **106,** 250 (1994).
24. Pierce, M. J., McClure, R. D., Welch, D. L., Racine, R. & van den Bergh, S. *New Perspectives on Stellar Pulsation and Pulsating Variable Stars, IAU Coll. 139* (eds Nemec, J. M. & Matthews, J. M.) 81 (Cambridge Univ. Press, 1992).
25. Welch, D. L. & Stetson, P. B. *Astr. J.* **105,** 1813 (1993).
26. Joner, M. D. & Taylor, B. J. *Publs astr. Soc. Pacif.* **102,** 1004 (1990).
27. Landolt, A. U. *Astr. J.* **104,** 340 (1992).
28. Lafler, J. & Kinman, T. D. *Astrophys. J. Suppl. Ser.* **11,** 216 (1964).
29. Burstein, D. & Heiles, C. *Astrophys. J. Suppl. Ser.* **54,** 33 (1984).
30. Freedman, W. L. *et al. Astrophys. J. Suppl. Ser.* **59,** 311 (1985).
31. Aaronson, M. *et al. Astrophys. J.* **302,** 536 (1986).
32. Dressler, A. *et al. Astrophys. J.* **313,** 43 (1987).
33. Capaccioli, M. *et al. Astrophys. J.* **350,** 110 (1990).
34. van den Bergh, S. *Publs astr. Soc. Pacif.* **104,** 861 (1992).
35. Rood, H. J., Page, T. L., Kinter, E. C. & King, I. R. *Astrophys. J.* **175,** 627 (1972).
36. VandenBergh, D. A. *The Formation and Evolution of Star Clusters, PASP Conf. Ser. 13* (ed. Janes, K.) 183 (Astr. Soc. Pacif., San Francisco, 1991).
37. van der Hulst, J. H., Skillman, E. D., Kennicutt, R. C. & Bothun, G. D. *Astr. Astrophys.* **177,** 63 (1987).
38. Cayatte, V., van Gorkom, J. H., Balkowski, C. & Kotanyi, C. *Astr. J.* **100,** 604 (1990).

ACKNOWLEDGEMENTS. Special thanks go the CFHT staff for their continued efforts to reduce local seeing effects, and to the DAO and CFHT staffs for their continued support of HRCam. We also thank the CFHT time allocation committees for their support of this effort and those observers who were forced to share nights with us during 1993 and 1994 for their patience. We thank G. Luppino, J. Tonry, S. Kwok and B. Hrivank for the use of a portion of their allocated time which allowed us to obtain our first two sets of images. CFHT is jointly operated by the National Research Council of Canada, CNRS of France and the University of Hawaii.

Competition for follicular niches excludes self-reactive cells from the recirculating B-cell repertoire

Jason G. Cyster, Suzanne B. Hartley* & Christopher C. Goodnow†

Department of Microbiology and Immunology, and † Howard Hughes Medical Institute, Beckman Center, Stanford University School of Medicine, Stanford, California 94305, USA

Two different approaches to follow clones of B lymphocytes in a diverse preimmune repertoire reveal a new process for eliminating self-reactive cells in the periphery which depends on competition between cells with different specificities. A key feature of this censoring mechanism is the selective exclusion of self-antigen-binding B cells from the normal migration route into lymphoid follicles, resulting in their premature death. This is a striking example of homeostasis by cellular competition for limiting niches and may explain the paradoxical association between immunodeficiency and autoimmunity.

BEFORE infection and exposure to new foreign antigens, a diverse preimmune repertoire of B lymphocytes continuously migrates between and through lymphoid tissues along defined routes[1–4]. After entering secondary lymphoid organs, preimmune B cells migrate briefly through T-cell-rich zones and then move into discrete B-cell-rich primary follicles for 12–24 hours before exiting into lymph or blood and recirculating[3,5–7]. In a healthy animal, the size of this B cell repertoire is tightly controlled, varying little from a mean of 2×10^8 cells in the mouse, the majority of cells being non-mitotic with a lifespan of more than four weeks[5,8–11]. Only a fraction of the 10^{11} possible antibodies generated by immunoglobulin gene rearrangement in the bone marrow[12] are therefore displayed at any one time as surface immunoglobulin (sIg) receptors on recirculating B cells. How the size and composition of this long-lived recirculating repertoire is controlled is of fundamental significance, because it is from this pool that antibody-forming cells are likely to be drawn immediately after infection. Moreover, deficits in follicular B cells accompany genetic and acquired immunodeficiencies[13], whereas excess B-cell accumulation in follicles characterize common human neoplasms such as follicular lymphoma[14,15].

To study the factors influencing entry and retention of particular B-cell clones in the preimmune repertoire, the frequency of B cells expressing a particular sIg specificity has been increased by engineering mice bearing rearranged immunoglobulin heavy chain (Hc) and light chain (Lc) transgenes[16–18]. This approach has confirmed that B cells that bind certain self-antigens undergo a cell-autonomous developmental arrest and are eliminated shortly after arising in the bone marrow[19–23]. Other self-antigen-binding B cells recirculate between lymphoid follicles but cannot mount antibody responses owing to an intrinsic change (anergy) that desensitizes sIg signalling[21,24–26]. The B-cell repertoire

* Present address: DNAX Research Institute, 901 California Ave, Palo Alto, CA 94304, USA.